Impurity Cluster Effects in High- and Low-Doping Semiconductor Materials

A. FERREIRA DA SILVA

Instituto de Física, Universidade Federal da Bahia, Campus Universitário de Ondina, 40210 340 Salvador, Bahia, Brazil

Received 27 January 2010; accepted 28 January 2010
Published online 8 July 2010 in Wiley Online Library (wileyonlinelibrary.com).
DOI 10.1002/qua.22633

ABSTRACT: The cluster-like impurity effect in semiconductor materials as Si, GaN, GaAs, and 4H—SiC for impurity concentrations spanning the metallic to the insulating regimes, i.e., from high- to low-doping concentration, has been investigated at low temperature. To metallic regime a critical impurity concentration for metal–nonmetal transition is estimated from a highly correlated system by a doubly doped H_2^+-like different impurity pairs. For insulating regime, the absorption measurements reveal low-energy absorption peaks identified as electronic transitions in three-donor clusters. The many-particle correlation via a multi-configurational self-consistent field model is used in the calculation. © 2010 Wiley Periodicals, Inc. Int J Quantum Chem 111: 1466–1471, 2011

Key words: molecule; donor pairs; donor triads; semiconductors; absorption

Introduction

The investigation of shallow atom-like impurity donors in Si, GaN, GaAs, and 4H—SiC semiconductor materials have attracted much interest as an important issue in the fabrication of optoelectronic and electronic devices, such as photovoltaic materials, blue-green light-emitting diodes, and high-temperature electronics. The efficiency of these devices is strongly affected by the incorporation of impurities. Experiments on doped semiconductors, above the impurity critical concentration N_c for the metal–nonmetal (MNM) transition, reveal a band gap variation even beyond 10% of the band gap of the pure material and below N_c at so-called noninteracting regime cluster of donors appear playing a reasonable role in the absorption measurements [1]. In the wake of recent measurements, we have showed and discussed the possible transitions involved in the present scenario.

In a lightly *n*-type doped semiconductor, the low-temperature spectroscopic measurements exhibit a series of atom-like lines which correspond to the optical transitions of isolated impurity atoms. As the impurity concentration increases, donor clusters rapidly become important. As the clusters get more dense, the absorption edge drops as one would expect that the donor clusters

Correspondence to: A. Ferreira da Silva; e-mail: ferreira@fis.ufba.br

Contract grant sponsor: CNPq and FAPESB (Brazilian Agencies).

will absorb at low energies, below the ionization and transition levels of the isolated impurities [2–5]. Above a certain critical doping concentration N_c, the donors (in *n*-type materials) spontaneously become ionized due to strong impurity–impurity interaction. This metallic regime is of great technological importance. We calculated this critical concentration from different models. A model is based on the Mott-Hubbard picture [1] of overlapping impurity electrons, assuming hydrogen-like wave functions. The other model is based on the metallic, strongly interacting impurity system i.e., Gutzwiller model [6]. These situations are schematically shown in Figure 1.

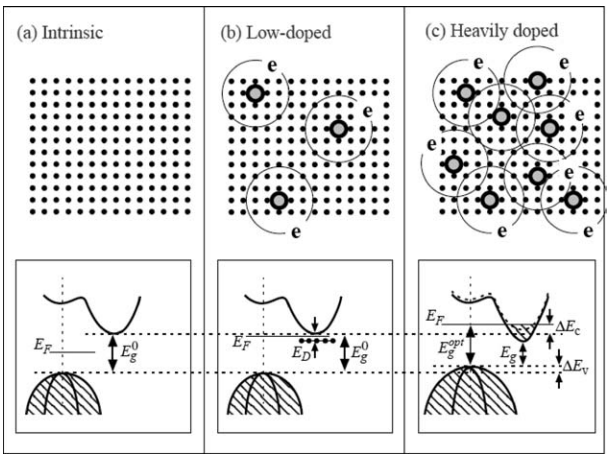

FIGURE 1. Schematic picture of the electronic band structure in *n*-type indirect transition materials. For direct transition, the bottom of conduction band lies just above the valence band. (a) The energy bands of the intrinsic material with completely occupied valence bands and completely unoccupied conduction bands. The upper panel shows schematically the crystalline structure (i.e., the atomic positions) and the lower panel shows the electronic band structure with the fundamental band gap energy E_g^0. E_F is the Fermi level. (b) At low-donor concentration, the donor electrons are localized hydrogen-like wave functions. The impurity electrons are almost noninteracting, forming localized, pairs, triads states a few meVs below the conduction band. (c) For heavy doping, the donor electrons strongly overlaps and the system gain energy by ionizing the donors and forming a corresponding electron gas, which will be above the critical concentration for a nonmetal metal transition. The conduction band minimum will be reduced by ΔEc and the valence band maximum by ΔEv (Ref. [1]).

High-Doping Regime

Through the use of a Mott-Hubbard tight-binding Hamiltonian, the impure density of states associated with it presents two sub-bands that overlap with increasing concentration. This would occur at an impurity concentration for which [6] $\Delta W/U = 1.15$, where ΔW is the unperturbed impurity band width in units of the ionization donor energy E_D, and U is the intraimpurity Coulomb interaction energy, also known as the Hubbard U, given by $U = 0.96 = E_D$ [6]. Such a scenario is well known as the Mott-Hubbard picture for the MNM transition. ΔW is related to the hopping integral energy T, between adjacent sites i and j, as $\Delta W = 2Z|T|$, Z is the coordination number for a particular arrangement of donor (SC, BCC, FCC, or diamond lattice). T is given by,

$$T = \int \psi_i(\mathbf{r}) H_1(\mathbf{r}) \psi_j(\mathbf{r}) d\mathbf{r} \tag{1}$$

and

$$U = \int d\mathbf{r}_1 d\mathbf{r}_2 \, |\psi(\mathbf{r}_i)|^2 |\psi(\mathbf{r}_2)|^2 \frac{e^2}{|\mathbf{r}_1 - \mathbf{r}_2|} \tag{2}$$

$H_1(\mathbf{r})$ is the one-particle Hamiltonian in the effective theory, including the kinetic energy operator and the Coulomb interaction of the positively charged donor ion electron. Ψ_j ($\mathbf{r}$–$\mathbf{R}_j$) is the simple hydrogenic wave function for the donor ground state at the randomly located site $\mathbf{R}_j$ (in units of a_D^*). Where the effective Bohr radius a_D^* is calculated from the ionization energy E_D of a single donor electron as the impurity electron wave function is assumed to be associated with only one conduction band (CB), that is, the many valley effects are neglected. It is given by,

$$a_D^* = \frac{e^2}{2\varepsilon(0) E_D} \tag{3}$$

The values of U and the donor impurity concentration N_D are both related to the ionization energy E_D. Using these equations, we calculate the values of the critical impurity concentration N_c.

We now consider in the calculation that the impurities are distributed over a regular lattice (SC, BCC, FCC, and diamond), averaging these different arrangements of the impurities. The

TABLE 1
Ionization energies, Bohr radia, and dielectric constants for 4H—SiC.

E_D (meV)	a_D^* (Å)	ε (0)
$E_1 = 52$	14.03	9.85
$E_2 = 92$	7.96	9.85

wave function considering the many-valley effect is given by

$$\psi_i(\mathbf{r}) = \frac{1}{\sqrt{v}} \sum_{l=1}^{v} F_1(\mathbf{r} - \mathbf{R}_i)\phi(\mathbf{r}) \tag{4}$$

associated with v equivalent CB minima, ϕ_l is the Bloch function at the lth minima and $F_l(\mathbf{r})$ is the screened hydrogenic wave function, or envelope 1s wave function. Equation (1) reduces to,

$$\tilde{T} = \frac{e^2}{\varepsilon a_0^*}[T + S/2] \Big/ \sqrt{v} \tag{5}$$

where $\varepsilon = \varepsilon(0)$ is the dielectric constant and S is the overlap integral given by

$$S = \int \psi(\mathbf{r})\psi(\mathbf{r} - \mathbf{R}_j)d\mathbf{r} \tag{6}$$

The MNM transition is calculated through the average of T as in Eq. (5) and we call it as the averaged Mott-Hubbard method.

For 4H—SiC, we have to take into account the two different ionization energies in its doping structure as described in Table I.

With these two ionization energies, we may find the Hubbard U as $U_1 = 50.2$ meV and $U_2 = 88.4$ meV, respectively from E_1 and E_2 with D_1 band separated from CB about 1.9 meV and D_2 band about 3.4 meV. Both D_1 and D_2 impurity bands are separated by 1.5meV. For these doubly ionization energy samples, the hopping and the overlap between nearest neighbors will consist of the following cases, E_1–E_1, E_1–E_2, E_2–E_2 pairs, and E_2–E_1 (not symmetric) pair. We are assuming an equal distribution of donors on substitutional sites. As the radius of the E_2 impurity wave function is smaller than that for E_1, the hopping and overlap for a E_1–E_1 pair will be the largest and the hopping and overlap for the E_2–E_2 pair will be smaller for a given impurity–impurity separation. As for the same impurity concentration N we will have two different ionization energies and Bohr radia, the question then arises which energy and Bohr radius to use for E_2 relative to E_1. To circumventing this question we assume a hydrogenic model with two different donor sites as follows. For the scheme represented in Figures 1 and 2, we may suppose that the E_1 band will play a major role on the thermodynamic and transport properties of the considered system. The Fermi energy E_F will remain between E_1 and both D_1 and D_2 bands, shifting to the right side with the increasing impurity concentration. E_2 will play a minor hole on those properties. We may use E_1 as our scaled energy for the doubly impurity sites system. Therefore, for two E_D's we can solve our T_{ij} for two different impurity sites as a H_2^+-like system.

We may identify in Figure 2, $E_2 = i$ and $E_1 = j$ and $R_{ij} = R_i$–R_j. The screening factors are $\alpha = \frac{1}{a_i^*}$ and $\beta = \frac{1}{a_j^*}$. As we know $E_D = \frac{7.2}{\varepsilon a_D^*}$ then $\beta = \frac{a_j^*}{a_i}\alpha$ or $\beta = \frac{E_D^i}{E_D^j}\alpha$.

For the doubly doped 4H—SiC material, we have $E_D^i = E_2 = 92meV \Rightarrow a_i^* = 7.96$Å, $E_D^j = E_1 = 52meV \Rightarrow a_j^* = 14.03$Å, and $\beta = 1.76\alpha$

Considering α and β, we can write Eq. (5) as,

$$\tilde{T}_{ij}^{\alpha,\beta}(R) = \frac{e^2}{\varepsilon\, a_j^*}\left[\left\langle T_{ij}^{\alpha,\beta}\right\rangle + \left\langle S_{ij}^{\alpha,\beta}\right\rangle/2\right] \Big/ \sqrt{v} \tag{7}$$

$\left\langle T_i^{\alpha.\beta}\right\rangle$ and $\left\langle S^{\alpha.\beta}\right\rangle$ are the averaged different arrangements of the donors and different types of hopping and overlaps (i.e., $T^{\alpha,\alpha}$, $T^{\alpha,\beta}$, $T^{\beta,\alpha}$, $T^{\beta,\beta}$ and $S^{\alpha,\alpha}$, $S^{\alpha,\beta}$, $S^{\beta,\alpha}$, $S^{\beta,\beta}$). For 4H—SiC $v$is equal to three [1].

In a real system the impurities will, of course, be randomly distributed. Here, we assume that the impurities are distributed over a regular lattice (SC, FCC, BCC, and Diamond structure) of

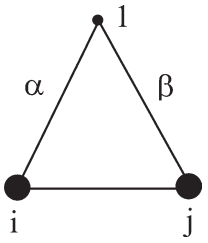

FIGURE 2. Schematic picture of a double-donor H_2^+-like pair impurity.

TABLE II

Critical concentrations for the MNM transition of *n*-type materials, calculated using two different methods (see text).

Materials	Dopant		E_D(meV)	Critical concentration N_c (cm^{-3}) ⟨Mott-Hubbard⟩	Spin susceptibility	Experiment
Si	P	*n*-type	45.5	3.4×10^{18}	3.5×10^{18}	3.7×10^{18}
GaN	O	n-type	33.2	1.2×10^{18}	—	1.0×10^{18}
GaAs	Si	*n*-type	5.3	1.6×10^{16}	—	—
4H—SiC	N	*n*-type	52 and 92	5.6×10^{18}	6.0×10^{18}	1.0×10^{19}

Measured critical concentrations are from Ref. [7] for Si:P, GaN from Ref. [1], and for 4H—SiC from Ref. [8].

the host material, and then average these different arrangements of impurities as well as the different types of hopping and overlap integrals.

The integrals for different type of donors are written as

$$T^{\alpha\beta} = \frac{4(\alpha\beta)^{3/2}}{(\alpha^2-\beta^2)^2 R}\left\{2\beta e^{-\alpha R} + \left[(\alpha^2-\beta^2)R^* - 2\beta\right]e^{-\beta R}\right\} \tag{8}$$

$$T^{\beta\alpha} = \frac{4(\alpha\beta)^{3/2}}{(\alpha^2-\beta^2)^2 R}\left\{\left[2\alpha + R(\alpha^2-\beta^2)\right]e^{-\alpha R} - 2\alpha e^{-\beta R}\right\} \tag{9}$$

$$T_{\alpha\alpha} = (1+\alpha R^*)e^{-\alpha R} \tag{10}$$

$$T_{\beta\beta} = (1+\beta R^*)e^{-\beta R} \qquad S_{\alpha\alpha} = S_{\beta\beta} = S \tag{11}$$

$$S = \frac{8(\alpha\beta)^{3/2}}{(\alpha^2-\beta^2)^3 R}\left\{\left[4\alpha\beta + (\alpha^2-\beta^2)\beta R\right]e^{-\alpha R} - \left[4\alpha\beta - (\alpha^2-\beta^2)\alpha R\right]e^{-\beta R}\right\} \tag{12}$$

$$S_{\alpha\alpha} = \left[1+\alpha R + (\alpha R)^2/2\right]e^{-\alpha R} \tag{13}$$

$$S_{\beta\beta} = \left[1+\beta R + (\beta R)^2/2\right]e^{-\beta R} \tag{14}$$

We have used the Gutzwiller scheme to calculate the MNM transition by a spin susceptibility calculation as the second model [6]. Following Ferreira da Silva [6], we may find the spin susceptibility at finite temperature T, χ_s as

$$\chi_s(T) = \eta_x(T)\chi_0(T) \tag{15}$$

where $\chi_0(T)$ is the Pauli spin susceptibility and $\eta_x(T)$ is an enhancement factor given by

$$\eta_x(T) = D(T)^{-1}\left\{1 - \frac{\chi_0(T)U[1+U/2U_0(T)]}{2\mu_B^2[1+U/U_0(T)]}\right\} \tag{16}$$

where,

$$D(T)^{-1} = \left\{1 - [U/U_0(T)]^2\right\}^{-1} \tag{17}$$

U is the Hubbard correlation energy or intradonor Coulomb interaction, μ_B the Bohr magnetron, $U_0(T)$ is a critical correlation energy as a function of the free energy at $U = 0$ and $D(T)^{-1} = m^*/m_0$ is identified as the effective mass with m_0 the bare mass. $U_0(T)$ and $\chi_0(T)$ are dependent of the new hopping integrals presented as Eq. (7). The spin susceptibility also depends on the material density ρ. For instance 4H—SiC $\rho = 3.166$ g/cm^3. The electronic effective mass will enhance χ_s(T) as the MNM is approached from the metallic side, with a dependence on U, as a result the spin susceptibility tends to diverge at the critical concentration for the MNM transition.

The calculated critical concentrations N_c for the different *n*-type materials are presented in Table II. Note that all the three computational methods give the same order of N.

LOW-DOPING REGIME

Work to date has concentrated on the search for optical transitions of donor impurities [1, 2, 9–13] once a peak appeared in the experimental investigations on the low-energy side of the 1*s* to 2*p* transition in Si, GaAs, GaN *n*-type doped semiconductors. The first attempt to explain such low-energy peak as arising from donor-cluster transitions were carried out by the Heitler-London approximation [14] and by Golka and Piela [15], who used a Hartree-Fock method [5]. However, these works did not explain the low-energy

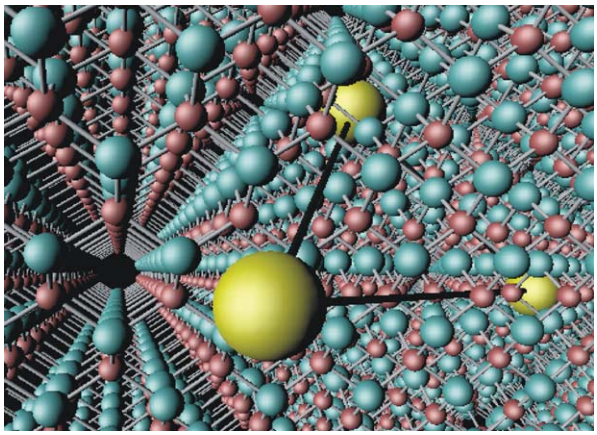

FIGURE 3. The donor-triad molecule cluster scheme in a host material. [Color figure can be viewed in the online issue, which is available at wileyonlinelibrary.com]

absorption peak. Canuto and Ferreira da Silva [3, 4] have improved the calculations through the dielectric function of the triad molecule using the self-consistent field (SCF) model obtaining results close to experimental findings.

We have investigated a donor-triad-cluster model, employing an ab initio multi-configurational self-consistent field (MCSCF) approach to electronic structure determination. Such a donor-triad scheme is shematically shown in Figure 3 in a GaAs or GaN host-like materials. For computational details (see Ref. [16]). The ionization energy from the H_3 transition corresponds to the energy required to promote one electron from the three-donor molecule to the bottom of the CB. As a multi-determinant description of the wave function is imperative to break chemical bonds, we expect the present ionization potential to be significantly improved for configurations with large interatomic distances. We show that using a full treatment of the electron correlation within the MCSCF, the sharp absorption line can be explained as electronic $H_3 \rightarrow H_3^+$ transitions in three-donor molecules.

For doped semiconductors, the effective Bohr radius $a_D^* = a_D/(E_D^* \times \varepsilon)$ is obtained from the experimental values of the ionization energy E_D^* and the low-frequency dielectric constant: ε(Si) = 11.7, ε(GaAs) = 12.4, ε(GaN) = 10.0, and ε(4H—SiC) = 9.85. The dielectric function $\varepsilon(\omega) = \varepsilon_1(\omega) + i\varepsilon_2(\omega)$ describes the optical response of the material, and it is directly related to the absorption $\alpha(\omega) = -\mathrm{Im}\langle\langle G(\omega,R)\rangle\rangle/\pi$, where $\langle\langle \ldots \rangle\rangle/\pi$, means average disorder of the Green's function propagator [3, 4, 16]. For the ground-state energies,

$$\alpha(\omega) = \int P(R)\delta(\nabla\omega - E_i^0(R))dR, \qquad (18)$$

where $E_i^0 = E^0(H_3^+) - E^0(H_3)$ is the ionization energy of the lowest state of the three-donor molecules. This ionization energy from the H_3 transition corresponds in our model to the energy required to promote one electron from the three-

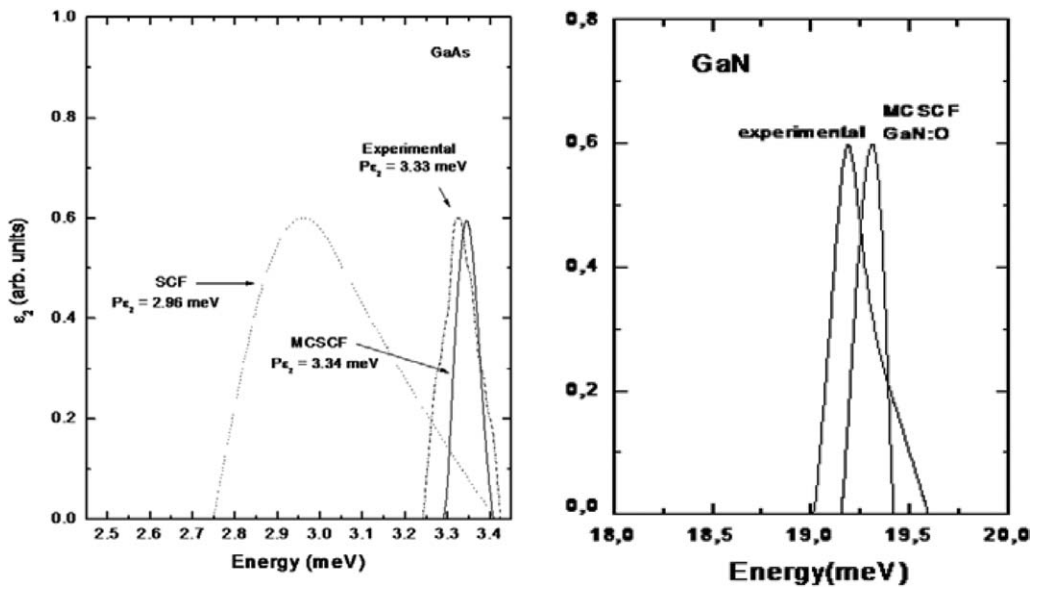

FIGURE 4. Imaginary part of the dielectric function for three-donor clusters in *n*-type GaAs and GaN. Experiments are from Ref. [2] for GaAs and Ref. [17] for GaN.

donor molecule to the bottom of the CB. $P(R)$ is the triad distribution function at separation R (see Refs. [3, 4, 14, 16]). The imaginary part $\varepsilon_2(\omega)$ of the dielectric function is obtained from

$$n(\omega) = n + \int \alpha(\omega)/2\pi(\omega'^2 - \omega^2)d\omega' \qquad (19)$$

$$\varepsilon_2(\omega) > 2\mathrm{Re}[n(\omega)]\mathrm{Im}[n(\omega)] \qquad (20)$$

The results for ε_2, which properly describes the positions of the absorption bands, are shown in Figure 4 for GaAs- and GaN-doped materials. The figure for GaAs material includes both the SCF [3, 4] and MCSCF model calculations applied to doped with Si. $P\varepsilon_2$ stands for the peak position.

The MCSCF calculation presents a sharper peak around the experimental results with less dispersion compared to the corresponding SCF result [3, 4]. According to Eq. (18), the MCSCF absorption peak should therefore be sharper and appear at a higher energy than the corresponding SCF peak, which is also observed in Figure 4. Thus, with a proper inclusion of the electron correlation in the three-donor cluster, we obtained a good agreement between the calculations and the experimental result for the $\varepsilon_2(\omega)$.

E_D^* and $E(1s–2p_\pm)$ transitions for shallow donor P in Si, O in GaN, Si in GaAs, and N in 4H—SiC i.e., Si:P, GaN:O, GaAs:Si [1, 9–13], and 4H—SiC:N [8] are $E_P^* = 45.5$ meV, $E_O^* = 33.23$ meV, $E_{Si}^* = 5.3$ meV, and $E_N^* = 91.8$ meV, respectively and the observed prominent peak, around 27.3 meV for Si:P, 19.2 meV for GaN:O, 3.0 meV for GaAs:Si, and 55.5 meV for 4H—SiC:N have these intensities following $E(\mathrm{Si}) = E_P^*(1s–2p_\pm)$, $E(\mathrm{GaAs}) = E_{Si}^*(1s\text{-}2p_\pm)$, $E(\mathrm{GaN}) = E_O^*(1s–2p_\pm)$, and $E(4\mathrm{H—SiC}) = E_N^*(1s–2p_\pm)$.

From n-type systems presented here, as well as from the systems in Refs. [9–13], we observe that the transitions are roughly related to $E(1s–2p_\pm) > 0.6E_D^*$. The calculated MCSCF peak energy $E(P\varepsilon_2)$ for the transition derived from the ionization energy of both oxygen in GaN and silicon in GaAs are in excellent agreement with the experimental finding of ~19.2 meV and ~3.0 meV [13, 2]. We predict a prominent peak of ~27 meV for phosphorous in Si in agreement with Ref. [18] and of ~55.5 meV for nitrogen in 4H—SiC.

Summary

In summary, we have shown that by using a donor pair as hydrogen-like impurity we can properly describe a MNM transition for single and doubly doped materials. For a low-doped regime, we have found that it is crucial to take into account the all-electron correlation in the optical absorption calculation of donor clusters in semiconductors. The observed low-energy peaks in Si:P, GaN:O, GaAs:Si, and 4H—SiC:N are identified as electronic transitions of triad clusters.

ACKNOWLEDGMENT

The author is in debt to Clas Persson for valuable discussions on the work and Figures 1 and 3.

References

1. Persson, C.; Ferreira da Silva, A. In Optoelectronic Devices: III-Nitrides; Razeghi, M.; Henini, M., Eds.; Elsevier Ltd: Oxford, UK, 2004; p 479.
2. Bajaj, K. K.; Birch, J. R.; Eaves, L.; Hoult, R. A.; Kirkman, R. F.; Simmonds, P. E.; Straddling, R. A. J Phys C 1975, 8, 530.
3. Ferreira da Silva, A.; Canuto, S. Solid State Commun 1990, 75, 939.
4. Canuto, S.; Ferreira da Silva, A. Phys Rev B 1993, 48, 18261.
5. Geim, A. K.; Foster, T. J.; Nogaret, A.; Mori, N.; McDonnell, P. J.; La Scala, N., Jr.; Main, P. C.; Eaves, L. Phys Rev B 1994, 50, R8074.
6. (a) Ferreira da Silva, A. Phys Rev B 1991, 43, 6551; (b) Ferreira da Silva, A. Phys Rev Lett 1987, 59, 1263.
7. Newman P. F.; Holcomb, D. F. Phys Rev Lett 1983, 51, 2144.
8. Ferreira da Silva, A.; Pernot, J.; Contreras, S.; Sernelius, B. E.; Persson, C.; Camassel, J. Phys Rev B 2006, 74, 245201.
9. Götz, W.; Johnson, N. M.; Chen, C.; Liu, H.; Kuo, C.; Imler, W. Appl Phys Lett 1996, 68, 3144.
10. Moore, W. J.; Freitas, J. A., Jr.; Molnar, R. J. Phys Rev B 1997, 56, 12073.
11. Mireles, F.; Ulloa, S. E. Appl Phys Lett 1999, 74, 248.
12. Wang, H.; Chen, A.-B. J Appl Phys 2000, 87, 7859.
13. Moore, W. J.; Freitas, J. A., Jr.; Braga, G. C. B.; Molnar, R. J.; Lee, S. K.; Lee, K. Y.; Song, I. J. Appl Phys Lett 2001, 79, 2570.
14. Nagasaka, K.; Narita, S. J Phys Soc Jpn 1973, 35, 797.
15. (a) Golka, J.; Piela, L. Solid State Commun 1977, 21, 691; (b) Golka, J.; Stoll, H. Solid State Commun 1980, 33, 1183.
16. Souza de Almeida, J.; da Silva, A. J.; Norman, P.; Persson, C.; Ahuja, R.; Ferreira da Silva, A. Appl Phys Lett 2000, 87, 7859.
17. Moore, W. J.; Freitas, J. A., Jr.; Lee, S. K.; Park, S. S.; Han, J. Y. Phys Rev B 2002, 65, 081201.
18. Thomas, G. A.; Capizzi, M.; DeRosa, F.; Bhatt, R. N.; Rice, T. M. Phys Rev 1981, B23, 5472.